

Enantioselective Detection, Bioactivity, and Degradation of the Novel Chiral Fungicide Oxathiapiprolin

Yingying Gao, Xuejun Zhao, Xiaofang Sun, Zhen Wang, Jing Zhang, Lianshan Li, Haiyan Shi, and Minghua Wang*



Cite This: *J. Agric. Food Chem.* 2021, 69, 3289–3297



Read Online

ACCESS |



Metrics & More



Article Recommendations



Supporting Information

ABSTRACT: Oxathiapiprolin is a novel chiral piperidine thiazole isooxazoline fungicide that contains a pair of enantiomers. An effective analytical method was established for the enantioselective detection of oxathiapiprolin in fruit, vegetable, and soil samples using ultraperformance liquid chromatography-tandem triple quadrupole mass spectrometry. The optimal enantioseparation was achieved on a Chiralpak IG column at 35 °C using acetonitrile and 0.1% formic acid aqueous solution (90:10, v/v) as the mobile phase. The absolute configuration of the oxathiapiprolin enantiomers was identified with the elution order of *R*-(-)-oxathiapiprolin and *S*-(+)-oxathiapiprolin by electron circular dichroism spectra. The bioactivity of *R*-(-)-oxathiapiprolin was 2.49 to 13.30-fold higher than that of *S*-(+)-oxathiapiprolin against six kinds of oomycetes. The molecular docking result illuminated the mechanism of enantioselectivity in bioactivity. The glide score (-8.00 kcal/mol) for the *R*-enantiomer was better with the binding site in *Phytophthora capsici* than the *S*-enantiomer (-7.50 kcal/mol). Enantioselective degradation in tomato and pepper under the field condition was investigated and indicated that *R*-(-)-oxathiapiprolin was preferentially degraded. The present study determines the enantioselectivity of oxathiapiprolin about enantioselective detection, bioactivity, and degradation for the first time. The *R*-enantiomer will be a better choice than racemic oxathiapiprolin to enhance the bioactivity and reduce the pesticide residues at a lower application rate.

KEYWORDS: oxathiapiprolin, enantioselective, absolute configuration, bioactivity, degradation

INTRODUCTION

In recent decades, the development of chiral pesticides with high activity and slow release has attracted widespread attention.¹ However, chiral pesticide enantiomers have the same physical and chemical properties, whereas in the chiral environment, enantioselective activity, toxicity, or environmental behavior occurs due to the specific recognition of the target enzyme.^{2–4} For instance, Zhang et al. investigated the *R*-enantiomer of prothioconazole, and its metabolite showed high bioactivity and low toxicity and was preferentially degraded in soil.⁵ Di et al. reported that the bioactivity and toxicity of *S*-(+)-isocarboxipropyl were significantly greater than those of *R*-(-)-isocarboxipropyl and found that the *R*-enantiomer was rapidly degraded in the rice cultivation system.⁶ Pan et al. observed that the *R*-zoxamide degraded faster than *S*-zoxamide in red and white wines during fermentation processes.⁷ Li et al. reported that the (1*R*,2*S*)-bitethanol and (1*R*,2*R*)-bitethanol were preferentially degraded in cucumbers.⁸ Therefore, the evaluation results of chiral pesticides with racemates are inaccurate and unscientific. It is necessary to study the enantioselective bioeffects and environmental behaviors of chiral pesticides at the enantiomer level to provide more accurate data for the food safety and environmental risk assessment. The continuous introduction of novel structural compounds would promote the proportion of chiral pesticides to surpass 40%.⁹ However, due to the limitation of the level of enantioseparation, merely 25% of chiral pesticides have been evaluated and used in the form of the pure enantiomer.¹⁰

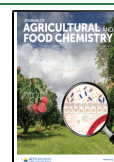
Oxathiapiprolin (1-(4-(4-((*S*)-5-(2,6-difluorophenyl)-4,5-dihydro-1,2-oxazol-3-yl)-1,3-thiazol-2-yl)-1-piperidyl)-2-(5-methyl-3-(trifluoromethyl)-1*H*-pyrazol-1-yl)ethanone) is a relatively new, widely used piperidinyli thiazole isooxazoline fungicide with the high bioactivity to oomycetes, which was developed by DuPont Agrochemical Company in 2012.^{11,12} Oxathiapiprolin plays an essential role in inhibiting oxysterol binding protein (OSBP) in oomycetes and exhibits excellent preventive and curative effects.^{11,13,14} The maximum residue limits (MRLs) for oxathiapiprolin in different agricultural products were established by the Codex Alimentarius Commission (CAC), and the range was 0.01–0.9 mg/kg. Moreover, the MRLs were recommended from 0.01 to 0.7 mg/kg in various matrixes from the European Union (EU), with representative MRLs of 0.01 mg/kg for pepper, 0.1 mg/kg for cucumbers, 0.2 mg/kg for tomato, and 0.7 mg/kg for grapes. So far, the MRLs of oxathiapiprolin have not been proposed for agricultural products in China.¹⁵ Oxathiapiprolin has a chiral carbon atom with two enantiomers (Figure 1). Currently, the studies of oxathiapiprolin mainly focused on the racemate. For example, the previous studies reported that

Received: July 1, 2020

Revised: January 19, 2021

Accepted: February 26, 2021

Published: March 12, 2021



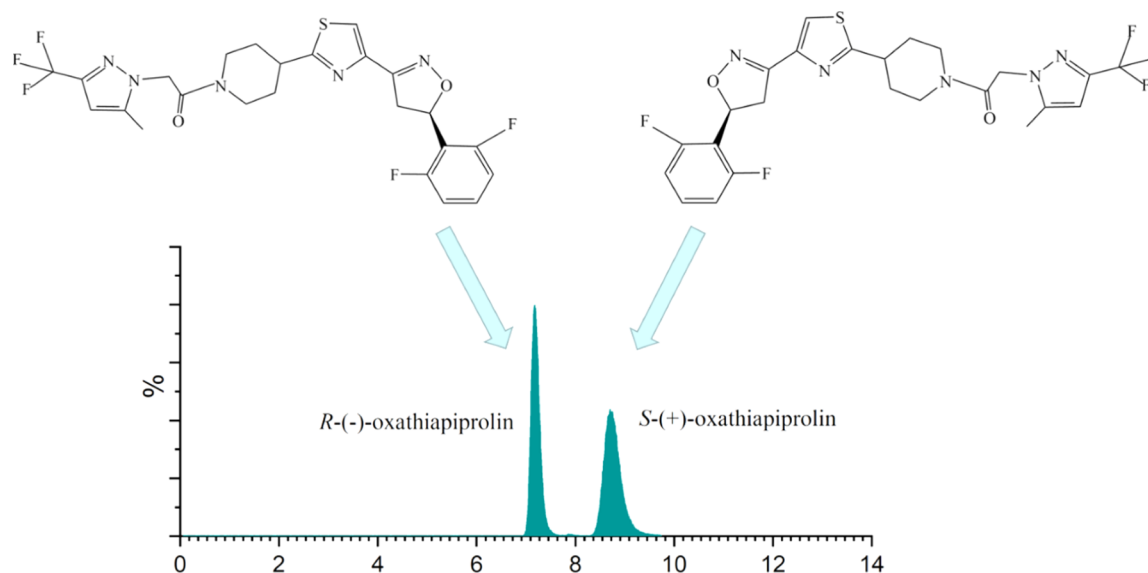


Figure 1. Chemical structure and typical MRM chromatograms of oxathiapiprolin enantiomers.

oxathiapiprolin was widely used to control oomycetes in vegetables, fruits, and tobaccos.^{16–18} Miao et al. reported that oxathiapiprolin showed excellent bioactivity on downy mildew caused by *Pseudoperonospora cubensis*.¹⁹ Peng et al. demonstrated the ability of oxathiapiprolin to activate plant disease resistance by inducing a targeted system of the *Pseudomonas syringae* pv. *tomato* and *Arabidopsis* interaction.²⁰ Oxathiapiprolin is toxic to aquatic fish, *Daphnia magna*, and algae, but there is no carcinogenicity, mutagenicity, or neurotoxicity in mammals at the recommended dosage.²¹ Wang et al. established the analysis methods for oxathiapiprolin and its main metabolites in cucumbers using HPLC-MS/MS.²² Ju et al. used the dispersive solid-phase extraction (DSPE) method combined with UHPLC-MS/MS to analyze oxathiapiprolin and its metabolites in a soil–water–sediment system.²³ However, the structure effect and environmental behavior of oxathiapiprolin at the chiral level are unclear. It is of great importance to investigate enantioseparation, bioactivity, and degradation behaviors for oxathiapiprolin at the enantiomer level to make a comprehensive and in-depth risk assessment for it.

In this work, an effective, rapid enantioseparation and detection method of oxathiapiprolin enantiomers was established using ultraperformance liquid chromatography-tandem triple quadrupole mass spectrometry (UPLC-MS/MS). The effects of chiral stationary phases (CSPs), mobile phase ratio, flow rate, and column temperature on oxathiapiprolin enantiomer separation were investigated. The absolute configuration of oxathiapiprolin enantiomers was identified by comparing experimental and calculated electron circular dichroism (ECD) spectra for the first time. Enantioselective bioactivity of the racemate oxathiapiprolin and single enantiomers against six kinds of pathogens was first explored. Molecular docking was used to explore combination differences between oxathiapiprolin enantiomers and target protein (OSBP). The optimized quick, easy, cheap, effective, rugged, and safe (QuEChERS) method was used for the sample extraction of pear, pepper, cucumber, tomato, and soil samples. The enantioselective degradation of oxathiapiprolin in tomato and pepper was investigated under field conditions. This work will provide a scientific and reasonable reference for the

possibility of a pure enantiomer to replace racemic oxathiapiprolin, which may show higher bioactivity and lower ecotoxicity, thereby conduct more accurate and reliable environmental monitoring and risk assessment.

MATERIALS AND METHODS

Reagents and Materials. Oxathiapiprolin (97.9% purity) was acquired from Dr. Ehrenstorfer (Augsburg, Germany). Oxathiapiprolin enantiomers (99.9% purity) were prepared by Chiralway Biotech Co., Ltd. (Shanghai, China). HPLC-grade acetonitrile was purchased from Merck (Darmstadt, Germany), and ultrapure water for HPLC/MS was purchased from Wahaha (Hangzhou, China). MS-grade formic acid was acquired from CNW Technologies, Inc. (Düsseldorf, Germany), and purified C18 and graphitized carbon black (GCB) were purchased from ANPEL Laboratory Technologies, Inc. (Shanghai, China), and 0.22 μm nylon syringe filters were purchased from Agela Technologies, Inc. (Agela, Tianjin, China). Other analytical-grade chemicals were purchased from commercial sources. The standard stock solutions of racemic oxathiapiprolin and the individual enantiomers (1000 mg/L) were dissolved in HPLC-grade acetonitrile and stored at 4 °C in the dark.

Instrumental Condition. The oxathiapiprolin enantiomer separation was investigated using a Waters ACQUITY UPLC system (Milford, MA, USA) in conjunction with a triple quadrupole mass spectrometer (Waters, USA) on Lux Cellulose-1, Lux Cellulose-2, and Lux Cellulose-3 (150 \times 2.0 mm, 3 μm) (Phenomenex, Guangzhou, China) and Chiralpak IG (250 \times 4.6 mm, 3 μm) (Daicel Chiral Technologies, Shanghai, China) columns. Acetonitrile and 0.1% formic acid aqueous solution (90:10, v/v) were used as the mobile phase at a flow rate of 0.6 mL/min. The injection volume was 5 μL , and the column temperature was maintained at 35 °C.

Data collection and analysis were carried out via Masslynx NT V.4.2 (Waters, USA) software. A triple quadrupole mass spectrometer equipped with an electrospray ion source in the positive mode (ESI⁺) was used for quantitative analysis of oxathiapiprolin enantiomers in the multiple reaction monitoring (MRM) mode. The mass spectrometry conditions consisted of a capillary voltage of 3.2 kV and source temperature and desolvation temperatures of 120 and 400 °C, respectively. Nitrogen (99.95%) was used as a desolvation gas at a rate of 1000 L/h and cone gas at 50 L/h. High-purity argon (99.99%) was used as the collision gas, with a pressure of 2×10^{-3} mbar in the T-wave cell. The optimized cone voltage was 11 V, and transitions of m/z 540.1 > 500.0 and m/z 540.1 > 167.0 were applied for quantification and identification with collision energies of 26 and 30 eV, respectively.

Optimization of Separation Conditions. To improve the enantioseparation sensitivity and efficiency, the types of CSPs (cellulose-based and amylose-based), mobile phase ratios (60:40, 70:30, 80:20, 90:10, 95:5; v/v), flow rates (0.4, 0.6, and 0.8 mL/min), and column temperatures (20, 25, 30, 35, and 40 °C) were investigated. The chromatographic separation parameters were calculated to evaluate the effects on enantioseparation, including the capacity factor (k), separation factor (α), and resolution (R_s) which were expressed as follows eqs 1–3. The thermodynamic parameters between enantiomers were also calculated using the following Van't Hoff equations eqs 4 and 5.^{2,8}

$$k = (t_R - t_0)/t_0 \quad (1)$$

$$\alpha = k_1/k_2 \quad (2)$$

$$R_s = 2(t_2 - t_1)/(w_2 + w_1) \quad (3)$$

$$\ln k = -\Delta H^\circ/RT + \Delta S^\circ/R + \ln \phi \quad (4)$$

$$\ln \alpha = -\Delta\Delta H^\circ/RT + \Delta\Delta S^\circ/R \quad (5)$$

where t_R is the retention time of enantiomers, t_0 is the void time, and w represents the peak width at half height. R and T represent gas constant and absolute temperature, respectively. ΔH° and ΔS° are the standard changes in enthalpy and entropy of the analytes from the mobile phase to the stationary phase, and ϕ is the phase ratio of the solid phase and the mobile phase. $\Delta\Delta H^\circ$ and $\Delta\Delta S^\circ$ were the ($\Delta H_2^\circ - \Delta H_1^\circ$) and ($\Delta S_2^\circ - \Delta S_1^\circ$) differences, respectively. When both $\Delta\Delta H^\circ$ and $\Delta\Delta S^\circ$ were positive, enantioseparation was entropy-driven; when they were negative, it was enthalpy-driven.

Determination of the Specific Optical Rotation. The specific optical rotation of oxathiapiprolin enantiomers was measured using an Autopol IV polarimeter (Rudolph Research Analytical, Hackettstown, NJ, USA) at 589 nm. The standard solutions for each enantiomer were 0.01 g/mL in acetonitrile and measured in triplicate at 20 °C.

Confirmation of the Absolute Configuration. The experimental ECD spectra were determined using a J815 circular dichroism spectropolarimeter (Jasco, Tokyo, Japan) at room temperature. The oxathiapiprolin enantiomers were dissolved in acetonitrile and placed in a 1 cm quartz cell, the scanning speed of the instrument was 50 nm/min in the range of 210–360 nm, and the average value of three scans was calculated. The experimental ECD spectra were drawn using Origin 2019 software.

The calculated ECD spectra of oxathiapiprolin enantiomers were predicted using the time-dependent density functional theory (TDDFT) method in conjunction with the DFT calculation at the level of B3LYP/6-31+G* using Gaussian 09 software.²⁴ The absolute configuration of oxathiapiprolin enantiomers was confirmed by comparing the experimental ECD spectra with the calculated ECD spectra.

Sample Extraction and Purification. After fully considering the effects of crop prevention and environmental protection, the five matrices (tomato, cucumber, pepper, pear, and soil) were used as the test samples in this study and were extracted and purified by the QuEChERS method.

Extraction. Approximately, 10 g of homogenized samples (tomato, cucumber, pepper, and pear) and soil samples were weighed into 50 mL Teflon centrifuge tubes. Formic acid water solution (5 mL, 2%) and 10 mL of acetonitrile were added. The mixtures were vortexed for 5 min at 2500 rpm and then ultrasonically extracted for 10 min. Next, 6 g of sodium chloride was added and vortexed for 5 min. Finally, the samples were centrifuged for 5 min at 4000 rpm to obtain the supernatant for purification.

Purification. The 1.5 mL supernatant was transferred into a 2 mL microcentrifuge tube containing 100 mg of C_{18} , 10 mg of GCB, and 150 mg of anhydrous $MgSO_4$. The tubes were sufficiently vortexed for 1 min and centrifuged for 5 min at 10,000 rpm. The purified liquid was collected and filtered through a 0.22 μ m nylon syringe filter for UPLC-MS/MS analysis.

Method Validation. The quantitative detection method of oxathiapiprolin enantiomers in the fruit, vegetable, and soil samples was evaluated by the specificity, linearity, matrix effect (ME), limit of quantification (LOQ), accuracy, and precision.

Five blank matrices were analyzed to verify the presence of interfering substances at the retention time of the target peaks. The solvent standard curve and matrix-matched calibration curves were fitted at 10–1000 μ g/L according to both the peak areas and the concentrations of each enantiomer in triplicate. The ME is ubiquitous in mass spectrometry, including the matrix enhancement effect and matrix suppression effect, which affects the quantitative analysis of compounds.^{6,15} External matrix-matched standards were used for both enantiomers to eliminate the ME that was based on guidelines published by the European Food Safety Authority (EFSA).²⁵ The ME was calculated according to eq 6:

$$ME = \frac{s_{\text{matrix}} - s_{\text{solvent}}}{s_{\text{solvent}}} \times 100\% \quad (6)$$

where s_{matrix} is the slope of the calibration curve in the matrix and s_{solvent} is the slope of the calibration curve in the solvent. If $-10\% < ME < 10\%$, the ME was nonsignificant. If $ME \leq -10\%$ or $ME \geq 10\%$, there was a significant matrix suppression effect or matrix enhancement effect.^{26,27}

The matrix-dependent LOQs of the oxathiapiprolin enantiomers in the agricultural products were defined as the lowest concentration level validated with satisfactory recoveries between 70 and 120%.

The accuracy and precision of the method in all matrices were measured by spiked recovery experiments. Five kinds of blank samples (tomato, cucumber, pepper, pear, and soil) were spiked with three concentrations in five replications for each oxathiapiprolin enantiomer at 10, 100, and 1000 μ g/kg. All spiked samples were vortexed for 1 min and allowed to stand for 2 h at room temperature. The spiked samples were then extracted and purified according to the abovementioned data. The accuracy and precision were verified by the mean recoveries and interday relative standard deviation (RSDs) and intraday RSDs.

Chiral Stability. The standard solution of the oxathiapiprolin enantiomers at 1 mg/L in methanol, acetonitrile, and water was stored at 4 and 25 °C to investigate the chiral inversion. The corresponding samples were collected at 0, 1, 3, 7, 14, 30, 60, 120, and 180 days and directly detected by UPLC-MS/MS.

Enantioselective Bioactivity of Oxathiapiprolin Enantiomers. Enantioselective bioactivity of oxathiapiprolin enantiomers against six kinds of pathogens was investigated by the mycelium growth rate method. The test pathogens, *Phytophthora capsici* (*P. capsici*), *Phytophthora melonis* (*P. melonis*), *Peronophythora litchi* (*Pe. litchi*), *Phytophthora sojae* (*P. sojae*), *Phytophthora infestans* (*P. infestans*), and *Phytophthora nicotianae* (*P. nicotianae*), were supplied by the College of Plant Protection, Nanjing Agricultural University (Nanjing, China). Serial concentrations of rac-oxathiapiprolin and two enantiomers (0.0625, 0.125, 0.25, 0.5, and 1 μ g/L) were added to the sterilized culture medium dissolved in acetone. The concentration of acetone in the culture medium was below 0.1%. The inocula (5 mm in diameter) from the margins of actively growing colonies were inoculated to pesticide-containing plates. Three replicates were performed for each concentration. The control was treated with 0.1% acetone. All the test plates were incubated at 25 ± 1 °C in darkness for 10 days. When the colony diameter of control reached about 70 mm, the diameters of all the test plates were measured by the cross method to calculate the inhibition rate. The inhibition rate was calculated using eq 7:

$$\text{inhibition rate} = \frac{D_{\text{control}} - D_{\text{treatment}}}{D_{\text{control}} - 5 \text{ mm}} \times 100 \quad (7)$$

where D_{control} is the colony diameter in the control and $D_{\text{treatment}}$ is the colony diameter in the treated sample.

Homology Modeling and Docking. Oxathiapiprolin is the first piperidinyl thiazole isoxazoline class of fungicides that acts by inhibiting with OSBP. In this study, the enantioselective interaction

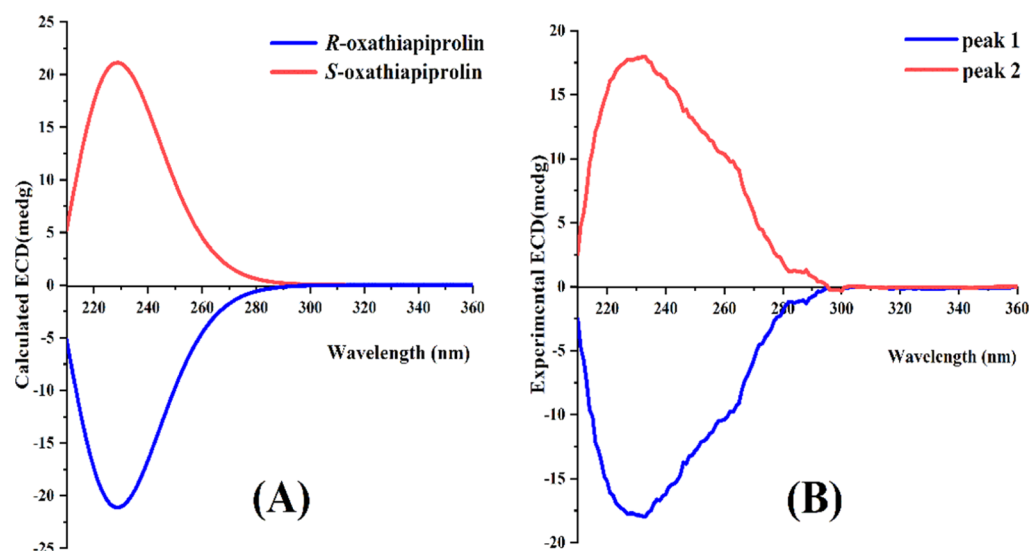


Figure 2. Calculated (A) and experimental (B) ECD spectra of oxathiapiprolin enantiomers.

between oxathiapiprolin and OSBP was investigated to explain the possible mechanism of bioactivity differences using homology modeling and molecular docking. At present, the OSBP of *P. capsici* had no single-crystal structure. Only Wu et al. reported that the structure of PsORP1 (Protein ID: 558498) in *P. capsici* was generated using the homology model application and SH2D was selected as the template.²⁸ Therefore, the protein preparation wizard module in Schrödinger software was used to preprocess it to construct the structure of PsORP1 in *P. capsici*. The Propka program was used to calculate the protonation status of each amino acid side chain at pH = 7, and the structure of the protein complex was optimized using the OPLS3 force field to obtain the best protein crystal structure. Before docking, the pesticide molecular structure was prepared and optimized using minimization by the LigPrep module. The glide module was used to dock the ligands into the active site of the proteins. The best glide score was applied to evaluate the binding modes between oxathiapiprolin enantiomers and protein. The glide score is negative for each docking complex conformation, so the larger absolute value of the glide score means a more stable combination between the ligand and receptor.

Enantioselective Degradation in Tomato and Pepper. Field degradation trials of oxathiapiprolin enantiomers were carried out in Nanjing (China). The fields had no application history of oxathiapiprolin. Each trial site was 30 m², with three test treatments and one control, and each plot had a buffer area of 1 m. The 10% oxathiapiprolin oil dispersion was sprayed at a dose of 44.445 g a.i./ha when the tomato and pepper grew to half of their full size. Approximately, 500 g of representative samples was collected from each plot at 2 h, 1, 2, 3, 5, 7, 14, and 21 d after spraying. All samples were subsequently homogenized and stored at -20 °C.

The first-order kinetics equation (eq 8) was applied to estimate the enantioselective degradation of oxathiapiprolin enantiomers in tomato and pepper. The half-life ($t_{1/2}$) of the enantiomers was calculated using eq 9. The enantiomeric fraction (EF) was used to evaluate the enantioselective degradation of oxathiapiprolin enantiomers in tomato and pepper using eq 10.

$$C_t = C_0 e^{-kt} \quad (8)$$

$$t_{1/2} = \ln 2/k = 0.693/k \quad (9)$$

$$EF = [R]/([R] + [S]) \quad (10)$$

where C_0 represents the initial concentration at 2 h after spraying, C_t represents the residual concentration in real time, k is the degradation rate constant, and $[R]$ and $[S]$ are the concentrations of R-(-)-oxathiapiprolin and S-(+)-oxathiapiprolin, respectively. The EF

value ranged from 0 to 1. If the EF was <0.5, the R-enantiomer was preferentially degraded, if the EF was >0.5, the S-enantiomer was preferentially degraded, and if the EF was 0.5, there was no enantioselective degradation.

RESULTS AND DISCUSSION

Enantioseparation of Oxathiapiprolin. Effect of the CSPs and Mobile-Phase Ratio on Enantioseparation. The CSPs is the key factor of chiral pesticide enantioseparation.²⁷ Among the four kinds of chiral columns, the oxathiapiprolin enantiomers could not be separated on Lux Cellulose-1 and Lux Cellulose-2 columns. Baseline separation was achieved on Lux Cellulose-3 and Chiralpak IG columns. Nevertheless, better enantiomeric resolution occurred on the Chiralpak IG column at a feasible retention time under the same conditions.

As an organic modifier, acetonitrile plays a key role in regulating retention time and Rs. The influence of the acetonitrile ratio (60–95%) on the separation of oxathiapiprolin was investigated on the Chiralpak IG column. The details of the enantioseparation parameters are summarized in Table S1. The Rs was improved with increasing acetonitrile content in the mobile phase. The two enantiomers could not achieve baseline separation with the proportion of acetonitrile 95%. However, when the acetonitrile proportion reached 60%, the retention time was more than 40 min. An excellent baseline resolution was achieved with Rs = 1.53 under the proportion of acetonitrile 90% in less than 12 min (Figure S1).

Effects of the Flow Rate and Column Temperature on Enantioseparation. The flow rate is another important factor affecting chiral separation according to the pressure of the system and retention time. As shown in Table S2, when the flow rate was increased from 0.4 to 0.8 mL/min, the analysis efficiency and retention time decreased significantly with increasing system pressure. When the flow rate was 0.6 mL/min, excellent resolution and shorter retention time for the two enantiomers were obtained with lower column pressure (Figure S2).

Temperature is another important parameter that affected the separation of chiral enantiomers. The temperature increase could reduce the density of the mobile phase and the viscosity, affecting the elution rate of the enantiomers. Moreover, the change in temperature affects the separation factor through the

Table 1. Linearity, Matrix Effect, and LOQ for Oxathiapiroline Enantiomers at 10–1000 $\mu\text{g/L}$

enantiomer	matrix	regression equation	R^2	ME (%)	LOQ ($\mu\text{g/kg}$)
R-oxathiapiroline	acetonitrile	$y = 444.02x - 599.71$	1		10
	tomato	$y = 374.62x + 339.53$	0.9957	-15.6	10
	pepper	$y = 321.35x + 914.20$	0.9998	-27.6	10
	cucumber	$y = 378.46x - 114.85$	0.9998	-14.8	10
	pear	$y = 394.3x + 825.66$	0.9999	-11.2	10
	soil	$y = 392.54x + 146.39$	0.9938	-11.6	10
S-oxathiapiroline	acetonitrile	$y = 449.14x - 677.63$	0.9999		10
	tomato	$y = 358.48x - 924.07$	0.9941	-20.2	10
	pepper	$y = 331.3x + 648.65$	0.9992	-26.2	10
	cucumber	$y = 380.85x - 145.81$	0.9998	-15.2	10
	pear	$y = 400.14x + 1061.4$	0.9997	-10.8	10
	soil	$y = 383.65x + 682.55$	0.9936	-14.6	10

Table 2. Accuracy and Precision for R-Oxathiapiroline and S-Oxathiapiroline in Five Matrices

enantiomer	matrix	spiked level ($\mu\text{g/kg}$)	intraday ($n = 5$)						interday ($n = 15$)
			day1		day2		day3		
			average recoveries (%)	RSD (%)	average recoveries (%)	RSD (%)	average recoveries (%)	RSD (%)	
R-oxathiapiroline	tomato	10	90.81	1.49	85.51	3.30	84.75	3.03	3.79
		100	104.75	1.82	102.21	1.66	101.63	3.45	1.61
		1000	96.37	3.46	94.18	2.70	91.00	2.37	2.87
	pepper	10	96.68	5.21	87.58	1.58	96.52	5.18	5.56
		100	97.44	4.68	95.59	2.28	92.91	2.03	2.39
		1000	104.28	6.25	108.02	5.11	97.91	3.57	4.94
	cucumber	10	100.63	2.84	97.91	4.79	104.54	2.53	3.30
		100	97.42	6.05	100.13	1.55	100.15	0.79	1.58
		1000	101.57	2.04	99.20	1.67	96.18	4.15	2.73
	pear	10	96.78	2.78	94.60	2.05	97.67	1.83	1.64
		100	102.55	1.45	106.06	5.66	106.28	3.60	1.99
		1000	104.62	3.54	101.51	3.68	105.80	1.12	2.13
	soil	10	75.05	1.93	76.43	2.19	79.26	1.84	2.79
		100	92.38	5.29	85.55	4.43	84.07	2.60	5.07
		1000	104.77	2.56	105.77	2.08	108.77	3.47	1.95
S-oxathiapiroline	tomato	10	91.29	3.57	86.21	1.91	86.65	2.76	3.20
		100	108.50	2.89	106.01	5.04	103.91	2.29	2.16
		1000	100.22	0.78	99.43	1.97	99.01	1.80	0.62
	pepper	10	104.99	1.89	96.93	3.77	99.16	4.12	4.14
		100	109.46	0.66	109.28	1.20	107.29	0.82	1.11
		1000	93.62	2.50	97.72	4.52	93.18	1.10	2.64
	cucumber	10	97.57	2.08	93.68	2.68	95.75	4.69	2.03
		100	93.28	2.97	94.52	2.30	97.74	1.95	2.42
		1000	100.73	3.65	95.16	3.33	96.18	3.48	3.05
	pear	10	95.63	1.81	92.39	3.65	101.64	4.55	4.86
		100	102.19	2.25	96.95	1.56	100.54	1.29	2.68
		1000	97.88	0.78	94.54	1.57	98.37	1.77	2.15
	soil	10	91.29	3.88	94.43	4.69	100.51	4.09	4.91
		100	108.50	5.78	97.71	2.64	98.02	1.41	6.06
		1000	90.56	4.24	83.95	2.23	91.87	1.05	4.78

thermodynamic effect, exacerbating the separation effect.^{29,30} The $\ln k$ or $\ln \alpha$ with $1/T$ had a good linearity, with correlation coefficients (R^2) between 0.9663 and 0.9788 at 20–40 °C. The separation efficiency of a pair of enantiomers improved when the column temperature was increased. The thermodynamic parameters of the oxathiapiroline enantiomers are summarized in Table S3. The fact that the values of $\Delta\Delta H^\circ$ and $\Delta\Delta S^\circ$ were positive indicated that there was entropy-driven separation. To establish an ideal chiral separation method and prolong the

chromatographic column lifetime, the appropriate detection temperature was 35 °C (Figure S3).

Specific Optical Rotation and Absolute Configuration of Oxathiapiroline Enantiomers. The specific optical rotations of peak 1 and peak 2 were $[\alpha]_D^{20} = -256.6^\circ$ and $[\alpha]_D^{20} = +256.4^\circ$ (acetonitrile, $c = 0.01$), respectively. As shown in Figure 2, the experimental ECD spectra of the oxathiapiroline enantiomers were similar to the calculated ECD spectra obtained by TDDFT calculations. According to the calculated and experimental ECD spectra combined with

specific rotation, we could correctly confirm the absolute configuration of the oxathiapiroprolin enantiomers from the Chiralpak IG column, as peak 1 was the *R*-(-)-oxathiapiroprolin and peak 2 was the *S*-(+)-oxathiapiroprolin.

Method Validation. *Specificity, Linearity, and LOQs.* There were no interference peaks near the retention time of the oxathiapiroprolin enantiomers in the blank samples (tomato, cucumber, pepper, pear, and soil). Table 1 summarized the solvent and matrix-matched standard calibration curves and R^2 values for each enantiomer in the five matrices. The two enantiomers of oxathiapiroprolin presented excellent linearity in the solvent and matrix-matched standard solutions in the range of 10–1000 $\mu\text{g}/\text{kg}$ with $R^2 \geq 0.9936$. The LOQs for oxathiapiroprolin enantiomers were 10 $\mu\text{g}/\text{kg}$.

Matrix Effect. The data in Table 1 indicated that the ME values were between -10.8 and -27.6%, which meant that there was a matrix suppression effect for both oxathiapiroprolin enantiomers in tomato, cucumber, pepper, pear, and soil. According to the EFSA guideline, the quantification of enantiomers could use matrix-matched standards for the method validation in complex matrices for nonisotopic labeled compounds.²⁵ Therefore, the matrix-matched calibration curves were used to eliminate the MEs of each enantiomer in the five matrices.

Accuracy and Precision. The mean recoveries and RSDs for oxathiapiroprolin enantiomers at three concentrations (10, 100, and 1000 $\mu\text{g}/\text{kg}$) on three consecutive days are summarized in Table 2. The mean recoveries were 75.05–109.46%, with intraday RSDs of 0.66–6.25% and interday RSDs of 0.62–6.06% in the five matrices. These data indicated that the method showed excellent accuracy and precision, so it is feasible to quantitatively detect the oxathiapiroprolin enantiomers in fruits, vegetables, and soil samples.

Stability of Oxathiapiroprolin Enantiomers. As shown in Figure S4, there was no significant change between the initial concentration and measured concentration at different times of oxathiapiroprolin enantiomers in acetonitrile, methanol, and water during 180 days. The results indicated that the configuration of chiral oxathiapiroprolin in acetonitrile, methanol, and water was stable, and chiral inversion was not observed. However, some synthetic pyrethroid chiral insecticides (permethrin, cypermethrin, and so on) were unstable in configuration under certain test conditions and could undergo chiral conversion in organic solvents.^{31,32} In addition, acetonitrile, methanol, and water are often used in sample preparation and extraction, so it is necessary to study whether chiral conversion exists in the solvent for chiral compounds. In this study, the configuration of oxathiapiroprolin enantiomers remained stable in acetonitrile, methanol, and water, and the results showed that the enantioselectivity was not caused by the instrument and solvent, which provided a reasonable theoretical basis for the chiral analysis of oxathiapiroprolin.

Enantioselective Bioactivity of Oxathiapiroprolin Enantiomers. There were significant bioactivity differences of the two oxathiapiroprolin enantiomers against six kinds of pathogens. The EC_{50} values of *rac*-oxathiapiroprolin and two enantiomers toward six kinds of pathogens are shown in Table 3. The bioactivity order of oxathiapiroprolin enantiomers for all test oomycetes was *R*-(-)-oxathiapiroprolin > *rac*-oxathiapiroprolin > *S*-(+)-oxathiapiroprolin (Figure 3). The results demonstrated that *R*-(-)-oxathiapiroprolin possessed more than 2.49–13.30 times bioactivity against six kinds of pathogens than *S*-(+)-oxathiapiroprolin. For example, the EC_{50} values for the *R*-

Table 3. Fungicidal Activity of *rac*-Oxathiapiroprolin and Enantiomers against Six Pathogens

test pathogens	compounds	R^2	EC_{50} ($\mu\text{g}/\text{L}$)	confidence intervals (95%)	S/R
<i>P. sojae</i>	<i>R</i>	0.9852	0.32	0.26–0.38	3.91
	<i>rac</i>	0.9947	0.40	0.35–0.45	
	<i>S</i>	0.9675	1.25	0.72–2.18	
<i>P. capsici</i>	<i>R</i>	0.9961	0.17	0.15–0.19	3.88
	<i>rac</i>	0.9909	0.24	0.21–0.29	
	<i>S</i>	0.9423	0.66	0.35–1.21	
<i>P. nicotianae</i>	<i>R</i>	0.9436	0.43	0.27–0.66	4.00
	<i>rac</i>	0.9690	0.54	0.38–0.78	
	<i>S</i>	0.9316	1.72	0.66–4.49	
<i>P. infestans</i>	<i>R</i>	0.9972	0.14	0.12–0.17	13.3
	<i>rac</i>	0.9949	0.22	0.19–0.25	
	<i>S</i>	0.9924	1.86	1.35–2.56	
<i>P. litchi</i>	<i>R</i>	0.9916	0.27	0.23–0.31	4.56
	<i>rac</i>	0.9946	0.74	0.62–0.87	
	<i>S</i>	0.9926	1.23	0.95–1.60	
<i>P. melonis</i>	<i>R</i>	0.9697	0.45	0.33–0.63	2.49
	<i>rac</i>	0.9755	0.84	0.56–1.25	
	<i>S</i>	0.9914	1.12	0.85–1.46	

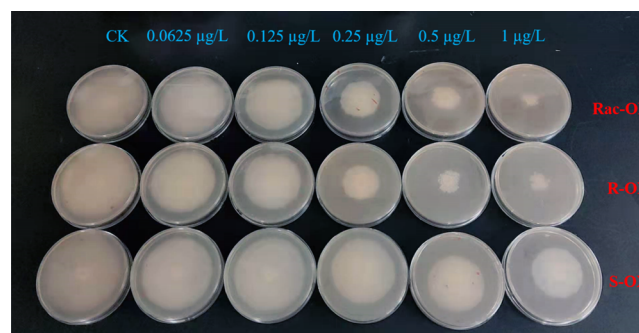


Figure 3. Enantioselective bioactivity of oxathiapiroprolin and its enantiomers against *P. sojae*.

and *S*-enantiomers were 0.14 and 1.86 $\mu\text{g}/\text{L}$ toward *P. infestans*, respectively.

The *R*-enantiomer exhibited two pi–pi force with LYS_260 and ARG_441 and a weaker aromatic H-bond with LEU_401. The *S*-enantiomer had a pi–pi force with ARG_236 and a H-bond with ALA_329. The results may be caused by changes in the spatial configuration of the molecule (Figure 4). In addition, the docking score of *R*-(-)-oxathiapiroprolin was -8.00 kcal/mol, while that of the *S*-enantiomer was -7.50 kcal/mol (Table S5). This meant that the *R*-enantiomer had a better binding ability to OSBP than the *S*-enantiomer in *P. capsici*. The results of molecular docking were in agreement with bioassay, indicating that the bioactivity of the *R*-enantiomer was superior to that of the *S*-enantiomer. These discoveries may provide an essential explanation for the differences in enantioselective bioactivity.

Enantioselective Degradation of Oxathiapiroprolin in Tomato and Pepper. As shown in Figure 5, the degradation of oxathiapiroprolin enantiomers in tomato and pepper fitted well with the first-order kinetic models. For tomato, the first-order kinetic equation of *R*-(-)-oxathiapiroprolin was $C = 0.9579 e^{-0.113t}$ with $R^2 = 0.9879$ and that of *S*-(+)-oxathiapiroprolin was $C = 0.9645 e^{-0.102t}$ with $R^2 = 0.9829$. The half-lives of *R*-(-)-oxathiapiroprolin and *S*-(+)-oxathiapiroprolin in tomato were 6.1 d and 6.8 d, respectively, and the difference was

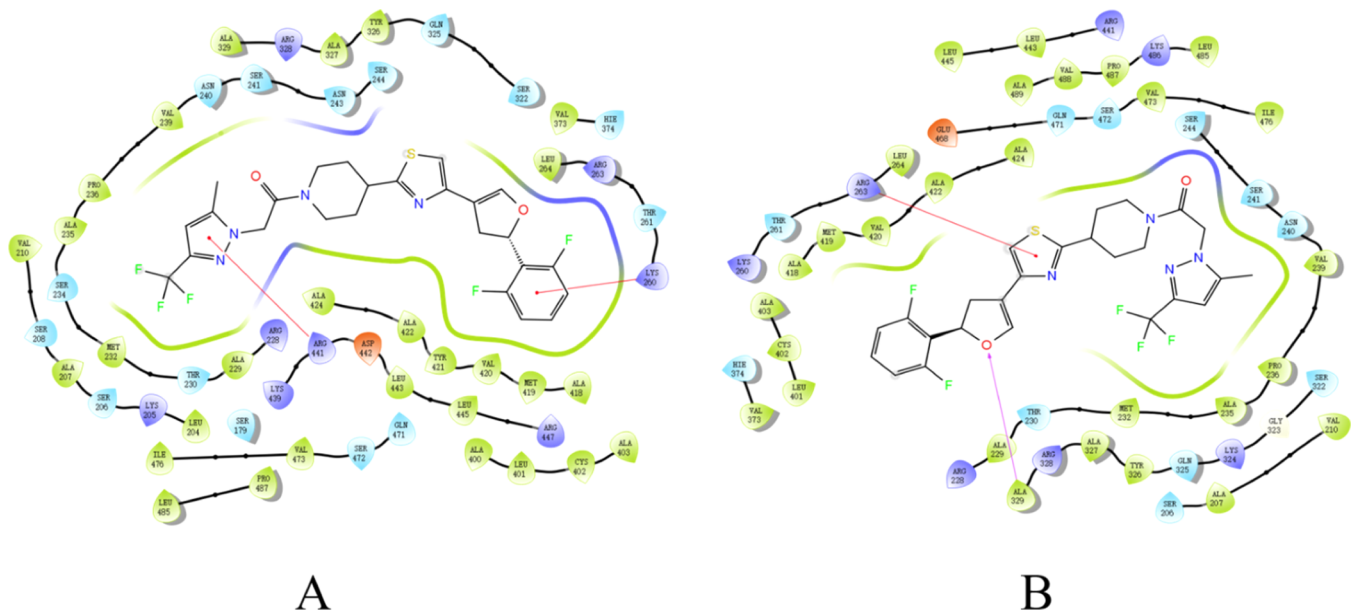


Figure 4. Enantiomer-specific binding modes for *R*-oxathiapiprolin (A) and *S*-oxathiapiprolin (B) bound to OSBP in *P. capsici*.

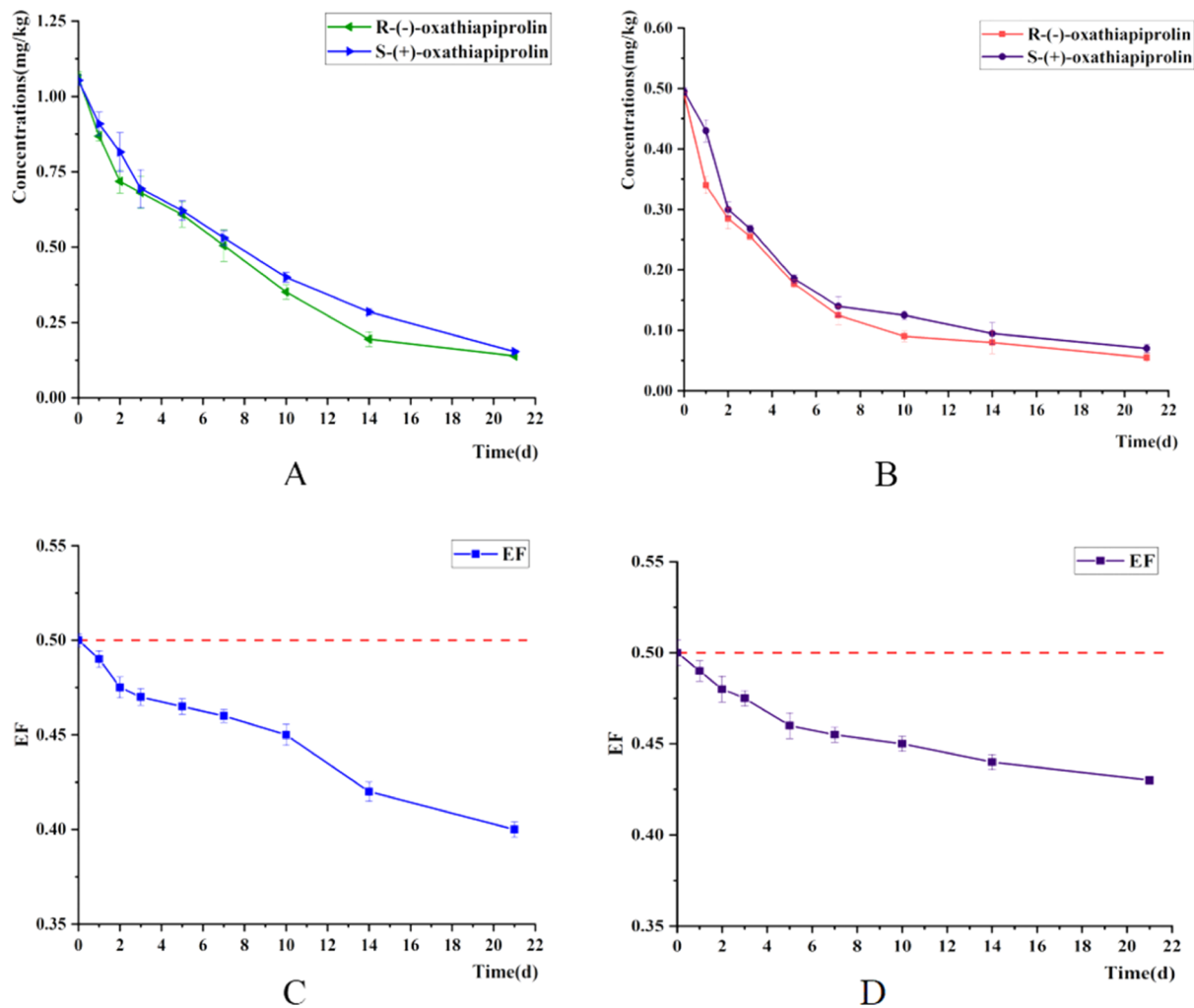


Figure 5. Degradation dynamics curves of tomato (A) and pepper (B); EF values of oxathiapiprolin enantiomers in tomato (C) and pepper (D).

significant ($P < 0.05$ according to Student's paired t -test). The EF values of oxathiapiprolin in tomato were 0.50 at 2 h and

0.40 at 21 d. For pepper, the half-life of *R*-(-)-oxathiapiprolin (3.1 d) was slightly shorter than that of *S*-(+)-oxathiapiprolin

(3.4 d). The degradation dynamics were $C = 0.4548 e^{-0.227t}$ ($R^2 = 0.9770$) and $C = 0.4932 e^{-0.205t}$ ($R^2 = 0.9503$) for the R- and S- enantiomers, respectively. The EF values decreased to 0.50 (at 2 h) from 0.43 (at 21 d), indicating that the R-enantiomer preferentially degraded in pepper ($P < 0.05$). Typical chromatograms of tomato and pepper samples are shown in Figure S5. The results were in accordance with that in grapes, showing a preferential degradation of R-(−)-oxathiapiprolin in tomato and pepper.³³ Until now, studies on the environmental behavior of oxathiapiprolin at the enantiomer level were still limited, mainly at the level of racemate.^{22,34} According to previous reports, enantioselective degradation of chiral pesticides in plants and environmental samples is widespread.^{35–37} Therefore, we speculated that the enantioselective degradation behavior of oxathiapiprolin in plants may be due to the different enzyme systems in plants, rather than due to instrumental and MEs. In the present study, R-(−)-oxathiapiprolin exhibited higher bioactivity in the six pathogens and a faster degradation rate in pepper and tomato. It may provide a reliable theoretical basis for the development of a single enantiomer to replace the racemate.

■ ASSOCIATED CONTENT

Supporting Information

The Supporting Information is available free of charge at <https://pubs.acs.org/doi/10.1021/acs.jafc.0c04163>.

Effects of acetonitrile ratio, temperature, and flow rate on enantioseparation; stability of oxathiapiprolin enantiomers; values of the grid score for oxathiapiprolin enantiomers by molecular docking; and typical chromatograms (PDF)

■ AUTHOR INFORMATION

Corresponding Author

Minghua Wang – Department of Pesticide Science, College of Plant Protection, State & Local Joint Engineering Research Center of Green Pesticide Invention and Application, Nanjing Agricultural University, Nanjing 210095, China;

orcid.org/0000-0001-5715-4981; Phone: +86 025 84395479; Email: wangmha@njau.edu.cn

Authors

Yingying Gao – Department of Pesticide Science, College of Plant Protection, State & Local Joint Engineering Research Center of Green Pesticide Invention and Application, Nanjing Agricultural University, Nanjing 210095, China

Xuejun Zhao – Department of Pesticide Science, College of Plant Protection, State & Local Joint Engineering Research Center of Green Pesticide Invention and Application, Nanjing Agricultural University, Nanjing 210095, China

Xiaofang Sun – Department of Pesticide Science, College of Plant Protection, State & Local Joint Engineering Research Center of Green Pesticide Invention and Application, Nanjing Agricultural University, Nanjing 210095, China

Zhen Wang – Department of Pesticide Science, College of Plant Protection, State & Local Joint Engineering Research Center of Green Pesticide Invention and Application, Nanjing Agricultural University, Nanjing 210095, China

Jing Zhang – Department of Pesticide Science, College of Plant Protection, State & Local Joint Engineering Research Center of Green Pesticide Invention and Application, Nanjing Agricultural University, Nanjing 210095, China

Lianshan Li – Department of Pesticide Science, College of Plant Protection, State & Local Joint Engineering Research Center of Green Pesticide Invention and Application, Nanjing Agricultural University, Nanjing 210095, China

Haiyan Shi – Department of Pesticide Science, College of Plant Protection, State & Local Joint Engineering Research Center of Green Pesticide Invention and Application, Nanjing Agricultural University, Nanjing 210095, China

Complete contact information is available at:

<https://pubs.acs.org/10.1021/acs.jafc.0c04163>

Funding

This study was supported by the National Key Research and Development Program of China (2016YFD0200207).

Notes

The authors declare no competing financial interest.

■ ABBREVIATIONS

UPLC-MS/MS, ultraperformance liquid chromatography tandem mass spectrometry; DSPE, dispersive solid-phase extraction; OSBP, oxysterol binding protein; CSPs, chiral stationary phases; ECD, electronic circular dichroism; TDDFT, time-dependent density functional theory; DFT, density functional theory; QuEChERS, quick, easy, cheap, effective, rugged, and safe; ME, matrix effect; LOQ, limit of quantification; S/N, signal-to-noise; RSD, relative standard deviation; EF, enantiomer fraction

■ REFERENCES

- (1) Qi, P.; Di, S.; Cang, T.; Yang, X.; Wang, X.; Wang, Z.; Xu, H.; Zhao, H.; Wang, X. Enantioselective behaviors of cis-epoxiconazole in vegetables-soil-earthworm system by liquid chromatography-quadrupole-time-of-flight mass spectrometry. *Sci. Total Environ.* **2020**, *706*, 136039.
- (2) Wen, Y.; Wang, Z.; Gao, Y.; Zhao, X.; Gao, B.; Zhang, Z.; Li, L.; He, Z.; Wang, M. Novel liquid chromatography-tandem mass spectrometry method for enantioseparation of tefluthrin via a Box-behnken design and its stereoselective degradation in soil. *J. Agric. Food Chem.* **2019**, *67*, 11591–11597.
- (3) Gao, B.; Zhang, Z.; Li, L.; Kaziem, A. E.; He, Z.; Yang, Q.; Qing, P.; Zhang, Q.; Wang, M. Stereoselective environmental behavior and biological effect of the chiral organophosphorus insecticide isofenphos methyl. *Sci. Total Environ.* **2019**, *648*, 703–710.
- (4) Xiang, D.; Qiao, K.; Song, Z.; Shen, S.; Wang, M.; Wang, Q. Enantioselectivity of toxicological responses induced by maternal exposure of cis-bifenthrin enantiomers in zebrafish (*Danio rerio*) larvae. *J. Hazard. Mater.* **2019**, *371*, 655–665.
- (5) Zhang, Z.; Gao, B.; Li, L.; Zhang, Q.; Xia, W.; Wang, M. Enantioselective degradation and transformation of the chiral fungicide prothioconazole and its chiral metabolite in soils. *Sci. Total Environ.* **2018**, *634*, 875–883.
- (6) Di, S.; Cang, T.; Qi, P.; Wang, X.; Xu, M.; Wang, Z.; Xu, H.; Wang, Q.; Wang, X. A systemic study of enantioselectivity of isocarboxiphos in rice cultivation: Enantioselective bioactivity, toxicity, and environmental fate. *J. Hazard. Mater.* **2019**, *375*, 305–311.
- (7) Pan, X.; Dong, F.; Liu, N.; Cheng, Y.; Xu, J.; Liu, X.; Wu, X.; Chen, Z.; Zheng, Y. The fate and enantioselective behavior of zoxamide during wine-making process. *Food Chem.* **2018**, *248*, 14–20.
- (8) Li, L.; Gao, B.; Zhang, Z.; Yang, M.; Li, X.; He, Z.; Wang, M. Stereoselective separation of the fungicide bitertanol stereoisomers by high-performance liquid chromatography and their degradation in cucumber. *J. Agric. Food Chem.* **2018**, *66*, 13303–13309.
- (9) Ye, J.; Zhao, M.; Liu, J.; Liu, W. Enantioselectivity in environmental risk assessment of modern chiral pesticides. *Environ. Pollut.* **2010**, *158*, 2371–2383.

- (10) Li, R.; Hu, M.; Liu, K.; Zhang, H.; Li, X.; Tan, H. Trace enantioselective determination of imidazolinone herbicides in various food matrices using a modified QuEChERS method and ultra-performance liquid chromatography/tandem mass spectrometry. *Food Anal. Methods* **2019**, *12*, 2647–2664.
- (11) Pasteris, R. J.; Hanagan, M. A.; Bisaha, J. J.; Finkelstein, B. L.; Hoffman, L. E.; Gregory, V.; Andreassi, J. L.; Sweigard, J. A.; Klyashchitsky, B. A.; Henry, Y. T.; Berger, R. A. Discovery of oxathiapiprolin, a new oomycete fungicide that targets an oxysterol binding protein. *Bioorg. Med. Chem.* **2016**, *24*, 354–361.
- (12) Wu, Q.; Zhao, B.; Fan, Z.; Guo, X.; Yang, D.; Zhang, N.; Yu, B.; Zhou, S.; Zhao, J.; Chen, F. Discovery of novel piperidinyl thiazole derivatives as broad-spectrum fungicidal candidates. *J. Agric. Food Chem.* **2019**, *67*, 1360–1370.
- (13) Miao, J.; Dong, X.; Lin, D.; Wang, Q.; Liu, P.; Chen, F.; Du, Y.; Liu, X. Activity of the novel fungicide oxathiapiprolin against plant-pathogenic oomycetes. *Pest Manage. Sci.* **2016**, *72*, 1572–1577.
- (14) Weber-Boyvat, M.; Zhong, W.; Yan, D.; Olkkonen, V. M. Oxysterol-binding proteins: functions in cell regulation beyond lipid metabolism. *Biochem. Pharmacol.* **2013**, *86*, 89–95.
- (15) Zhang, X.; Sun, H.; Wang, X.; Li, X.; Zhong, Q.; Luo, F.; Chen, Z. Enantioselective residue analysis of oxathiapiprolin and its metabolite in tea and other crops by ultra high performance liquid chromatography tandem mass spectrometry. *J. Sep. Sci.* **2020**, *43*, 3856.
- (16) Cohen, Y. The novel oomycide oxathiapiprolin inhibits all stages in the asexual life cycle of *Pseudoperonospora cubensis*-causal agent of cucurbit downy mildew. *PLoS One* **2015**, *10*, No. e0140015.
- (17) Bittner, R. J.; Mila, A. L. Effects of oxathiapiprolin on *Phytophthora nicotianae*, the causal agent of black shank of tobacco. *Crop Prot.* **2016**, *81*, 57–64.
- (18) Qu, T.; Grey, T. L.; Csinos, A. S.; Ji, P. Translocation of oxathiapiprolin in bell pepper plants and systemic protection of plants against *Phytophthora* Blight. *Plant Dis.* **2016**, *100*, 1931–1936.
- (19) Miao, J.; Dong, X.; Chi, Y.; Lin, D.; Chen, F.; Du, Y.; Liu, P.; Liu, X. *Pseudoperonospora cubensis* in China: Its sensitivity to and control by oxathiapiprolin. *Pestic. Biochem. Physiol.* **2018**, *147*, 96–101.
- (20) Peng, Q.; Wang, Z.; Liu, P.; Liang, Y.; Zhao, Z.; Li, W.; Liu, X.; Xia, Y. Oxathiapiprolin, a novel chemical inducer activates the plant disease resistance. *Int. J. Mol. Sci.* **2020**, *21*, 1223.
- (21) European Food Safety Authority. Peer review of the pesticide risk assessment of the active substance oxathiapiprolin. *EFSA J.* **2016**, *14*, No. e04504.
- (22) Wang, W.; Teng, P.; Liu, F.; Fan, T.; Peng, Q.; Wang, Z.; Hou, T. Residue analysis and risk assessment of oxathiapiprolin and its metabolites in cucumbers under field conditions. *J. Agric. Food Chem.* **2019**, *67*, 12904–12910.
- (23) Ju, C.; Dong, F.; Liu, X.; Wu, X.; Zhao, H.; Zheng, Y.; Xu, J. Rapid residue analysis of oxathiapiprolin and its metabolites in typical Chinese soil, water, and sediments by a modified quick, easy, cheap, effective, rugged, and safe method with ultra-high performance liquid chromatography and tandem mass spectrometry. *J. Sep. Sci.* **2015**, *38*, 909–916.
- (24) Tedesco, D.; Pistozzi, M.; Zanasi, R.; Bertucci, C. Characterization of the species-dependent ketoprofen/albumin binding modes by induced CD spectroscopy and TD-DFT calculations. *J. Pharm. Biomed. Anal.* **2015**, *112*, 176–180.
- (25) Bura, L.; Friel, A.; Magrans, J.; ParraMorte, J.; Szentes, C.; European Food Safety Authority. Guidance of EFSA on risk assessments for active substances of plant protection products that have stereoisomers as components or impurities and for transformation products of active substances that may have stereoisomers. *EFSA J.* **2019**, *17*, No. e05804.
- (26) Zhu, Y.; Liu, X.; Xu, J.; Dong, F.; Liang, X.; Li, M.; Duan, L.; Zheng, Y. Simultaneous determination of spirotetramat and its four metabolites in fruits and vegetables using a modified quick, easy, cheap, effective, rugged, and safe method and liquid chromatography/tandem mass spectrometry. *J. Chromatogr. A* **2013**, *1299*, 71–77.
- (27) Zhang, Z.; Zhou, L.; Gao, Y.; Zhang, J.; Gao, B.; Shi, H.; Wang, M. Enantioselective detection, bioactivity, and metabolism of the novel chiral insecticide fluralaner. *J. Agric. Food Chem.* **2020**, *68*, 6802–6810.
- (28) Wu, Q.-F.; Zhao, B.; Fan, Z.-J.; Zhao, J.-B.; Guo, X.-F.; Yang, D.-Y.; Zhang, N.-L.; Yu, B.; Kalinina, T.; Glukhareva, T. Design, synthesis and fungicidal activity of isothiazole-thiazole derivatives. *RSC Adv.* **2018**, *8*, 39593–39601.
- (29) Zhang, H.; Wang, X.; Wang, X.; Qian, M.; Xu, M.; Xu, H.; Qi, P.; Wang, Q.; Zhuang, S. Enantioselective determination of carboxyl acid amide fungicide mandipropamid in vegetables and fruits by chiral LC coupled with MS/MS. *J. Sep. Sci.* **2014**, *37*, 211–218.
- (30) Pan, X.; Dong, F.; Chen, Z.; Xu, J.; Liu, X.; Wu, X.; Zheng, Y. The application of chiral ultra-high-performance liquid chromatography tandem mass spectrometry to the separation of the zoxamide enantiomers and the study of enantioselective degradation process in agricultural plants. *J. Chromatogr. A* **2017**, *1525*, 87–95.
- (31) Liu, W.; Qin, S.; Gan, J. Chiral stability of synthetic pyrethroid insecticides. *J. Agric. Food Chem.* **2005**, *53*, 3814–3820.
- (32) Qin, S.; Gan, J. Abiotic enantiomerization of permethrin and cypermethrin: effects of organic solvents. *J. Agric. Food Chem.* **2007**, *55*, 5734–5739.
- (33) Liu, Q.; Dong, F.; Xu, J.; Liu, X.; Wu, X.; Li, R.; Jiang, D.; Wu, X.; Liu, Y.; Zheng, Y. Enantioselective separation and dissipation monitoring of oxathiapiprolin in grape using supercritical fluid chromatography tandem mass spectrometry. *J. Sep. Sci.* **2020**, *43*, 4077.
- (34) Yu, P.; Jia, C.; Zhao, E.; Chen, L.; He, H.; Jing, J.; He, M. Determination of oxathiapiprolin concentration and dissipation in grapes and soil by ultrahigh-performance liquid chromatography–tandem mass spectrometry. *J. Sci. Food Agric.* **2017**, *97*, 3294–3299.
- (35) Dong, F.; Li, J.; Chankvetadze, B.; Cheng, Y.; Xu, J.; Liu, X.; Li, Y.; Chen, X.; Bertucci, C.; Tedesco, D.; Zanasi, R.; Zheng, Y. Chiral triazole fungicide difenoconazole: absolute stereochemistry, stereoselective bioactivity, aquatic toxicity, and environmental behavior in vegetables and soil. *Environ. Sci. Technol.* **2013**, *47*, 3386–3394.
- (36) Lv, T.; Carvalho, P. N.; Casas, M. E.; Bollmann, U. E.; Arias, C. A.; Brix, H.; et al. Enantioselective uptake, translocation and degradation of the chiral pesticides tebuconazole and imazalil by *Phragmites australis*. *Environ. Pollut.* **2017**, *229*, 362–370.
- (37) Wang, Z.; Liu, S.; Zhao, X.; Tian, B.; Sun, X.; Zhang, J.; Gao, Y.; Shi, H.; Wang, M. Enantioselective separation and stereoselective dissipation of the novel chiral fungicide pydiflumetofen by ultra-high-performance liquid chromatography tandem mass spectrometry. *Ecotoxicol. Environ. Saf.* **2021**, *207*, 111221.